NEUTRONIC ANALYSIS OF AN ADS FUELLED WITH MINOR ACTINIDE AND DESIGNED FOR SPENT FUEL ENRICHMENT AND FISSILE FUEL PRODUCTION

by

***Busra DURMAZ*[1], *Gizem BAKIR*[2], *Alper Bugra ARSLAN*[3], *and Huseyin YAPICI*[1*]**

[1]Faculty of Engineering, Erciyes University, Kayseri, Turkey
[2] Faculty of Technology, Cumhuriyet University, Sivas, Turkey
[3] Faculty of Engineering and Architecture, Batman University, Batman, Turkey

Scientific paper
https://doi.org/10.2298/NTRP2104299D

This paper presents analyses of enrichments of uranium taken out from Canada Deuterium Uranium and pressurized water reactors spent fuels and fissile fuel breeding from thorium in two different helium cooled-accelerator driven system designs, DESIGN A and DESIGN B. In the beginning, the ^{235}U percentages in the uranium fuels taken out from the reactors spent fuels are 0.17 % and 0.91 %, respectively. Both system cores are fuelled with two different minor actinides compositions extracted from PWR-MOX spent fuels. The DESIGN A has one transmutation zone (enrichment zone) surrounding the fuel core and containing thorium or spent uranium fuels, while DESIGN B has a second transmutation zone (fissile fuel breeding zone) surrounding the first transmutation zone and containing only thorium fuel. In brief, a total of ten cases formed by the combinations of accelerator driven system designs, minor actinides components, and spent uranium with thorium fuels are analysed, which are six in DESIGN A containing one transmutation zone and four in DESIGN B containing two transmutation zones. Lead-bismuth eutectic alloy, a liquid heavy metal, consisting of 45 % lead and 55 % bismuth is used as target material in the investigated accelerator driven system. It is assumed that the target is bombarded with $1.2383\cdot10^{17}$ protons per second and that the energy of each proton is 1000 MeV. This means a proton beam power of 20 MW. The 3-D and time-dependent neutronic analyses are conducted by using the MCNPX 2.7 and CINDER 90 nuclear code. Both accelerator driven system designs are operated until the values of keff rise to 0.985 to determine the longest operation times that are the effective burn times in all cases.

Depending on the design, minor actinide composition, and fuel type (spent UO_2 and ThO_2), the results obtained at the end of cycle exhibit the effective burn times vary from 300 days to 2050 days, the fuel enrichments can reach up to 2.49-4.23 % and the values of gain reach up to 10.8-25.1.

Key words: accelerator-driven system, thermal reactor, spent fuel enrichment, thorium utilization

INTRODUCTION

Nowadays, pressurized water reactor (PWR) and Canada Deuterium Uranium reactor (CANDU) reactors based on uranium fuel produce the most of nuclear electricity. Commercial nuclear reactors cause the production of highly radioactive materials as high-level waste which mainly consists of minor actinides (MA) and long-lived fission products and managing these products is an issue for most countries. Currently, most nuclear countries take the *wait and see* approach for spent nuclear fuel management. On the other hand, these wastes (these spent fuels) contain significant amounts of fertile fuel which is not able to produce energy directly but can transmute into fissile fuel and generate energy.

Firstly, Rubia *et al*. [1] suggested accelerator driven system (ADS), which is an innovative reactor, for incineration of nuclear waste, utilization of thorium, and as an energy amplifier. Many nuclear scientists suggest that ADS can be an alternative solution to the deep geological disposal of nuclear waste. The same as transmutation of nuclear waste, these systems can generate large amounts of energy by using nuclear waste containing valuable fuel. Furthermore, they can breed fissile fuel from fertile fuels (such as ^{232}Th) via neutron capture reactions.

Gohar *et al*. [2] perform a study on spent fuel transmutation in a conceptual ADS. They use MCNP and Serpent code for analysing minor actinide trans-

* Corresponding author; e-mail: yapici@erciyes.edu.tr

mutation and their results show that 25.1 and 24.5 tons of minor actinides can consume for 35 full power years. Yapici [3-5] and Yapici *et al*. [6-8], examine spent fuel rejuvenation in fusion-fission reactors by using spent fuels discharged from various reactors. Yang *et al*. [9] study on minor actinide transmutation in ADS by using COUPLE3.0. Supplier-to-burner support ratio indicates what quantity of supplier reactors can be supported by a burner reactor and they find that the efficient transmutation supplier-to-burner support ratio is 28. Rodrigues *et al*. [10] study on ANICCA and several codes for the transmutation of MA, and they accomplish a reduction of MA by around 60 %. Liu *et al*. [11] work on the transmutation of MA in a lead-cooled fast reactor (LFR), and they exhibit that after MA transmute in LFR, the fraction of plutonium isotopes is about 85 %. Liu *et al*. [12] carried out a study on the AP1000 reactor, and their results show that it can burn 44.0 kg MA nuclides after a one-year fuel cycle. Zhou *et al*. [13] use ADS fuelled with spent PWR fuels, the transmutation of MA is flexible in the ADS system as seen in their results. Arslan *et al*. [14] perform a study on conceptual helium gas-cooled ADS fuelled with spent fuel extracted from CANDU and PWR which is investigated in three different cases. They use MCNPX 2.7 and CINDER 90 for numerical analyses, and they exhibit that significant amounts of spent fuel can be transmuted in their design.

Reserves of thorium element are approximately three times more than reserves of uranium element. In ADS or some types of reactors can be bred the ^{233}U fissile fuel from ^{232}Th isotopes with neutron capture reactions. Thus, thorium is a candidate to be an attractive fuel for nuclear reactors in the near future and many researchers work intensively on thorium utilization nowadays. Bakir *et al*. [15] investigate thorium utilization in ADS by using it with mixed oxide (MOX) spent fuel. Their study shows that ^{233}U of 155.1 g per day and ^{239}Pu of 103.6 g per day can be bred in their conceptual ADS. Bakir and Yapici [16] investigate thorium utilization in a D-T fusion breeder reactor fuelled with a mixture of natural UO_2 and ThO_2. They use MONTEBURN and MCNP codes separately, and they show that the neutronic results are very near each other for both codes. Their results also bring out that the D-T fusion reactor has high performance in terms of thorium utilization. Ali *et al*. [17] investigate thorium fuel utilization in ADS by using uranium mononitride (UN), UO_2 (seed fuel), and ThO_2 fuel. In their results reprocessed seed fuel and ThO_2 fuel is the best option for ^{233}U production while thorium fuel with the UN is the best case in terms of the longest cycle length. Kral *et al*. [18] work on thorium utilization in ADS experimental by using QUINTA spallation set-up and they validate with MCNP code. They found that both results are in very good agreement and maximum (n γ) reaction is obtained in the centre of their system's target. Zhu *et al*. [19] compare thorium blanket system and pebble bed fluoride salt-cooled high temperature reactor (PB-FHR) in terms of thorium utilization. In their results, they found that the pebble mixing system in PB-FHR has a bit lower thorium transmutation performance than the thorium blanket system. Yang *et al*. [20] investigated thorium-based molten salt fast energy amplifier (TMSFEA) for energy production and thorium utilization and their results showed that they obtain efficient thorium utilization in their system. Qaaod *et al*. [21] investigated the transuranic elements transmutation and transmutation of different configurations of fuel elements with MA in an ADS. They designed two-zone model which comprises a fast neutron spectrum and thermal neutron spectrum for the inner and outer zone, respectively. They coupled the subcritical core with an external deuterium-tritium source (14 MeV energy). Their results showed that most of the actual minor actinide isotopes transmuted effectively in the inner fast spectrum zone of the ADS.

Unlike our work in [14-16], this study presents the enrichment of uranium fuels extracted from spent fuels of PWR and CANDU reactors in an ADS fuelled with only MA compounds, without using any enriched fresh fuel and the production of fissile fuel from thorium.

CONCEPTUAL ADS DESIGNS

The main purpose of this study is, without using any enriched fresh fuel in an ADS, fuelled with MA compositions, to enrich the uranium fuels extracted from spent fuels of PWR and CANDU reactors and to produce fissile fuel from thorium. For this purpose, two different helium-cooled ADS (DESIGN A and DESIGN B), fuelled with MA compositions extracted from PWR-MOX spent fuel, are designed conceptually. The ADS are reactors operating sub-critically and generally consist of four parts: LBE-spallation neutron target, Sub-critical fuel zone, Transmutation zone, and Reflector zone. Their main task is the transmutation of radioisotopes. As is apparent from fig. 1, two different helium-cooled ADS are designed conceptually as DESIGN A and DESIGN B. Lead-Bismuth Eutectic alloy, a liquid heavy metal, consisting of 45 % Lead and 55 % Bismuth is used in both ADS designs as the spallation neutron target. The cores of both ADS designs are fuelled with the MA compositions extracted from PWR-MOX. While DESIGN A has one transmutation zone (fuel enrichment zone, FEZ1) surrounding the MA fuel core and includes ThO_2 or spent UO_2 fuels, DESIGN B has a second transmutation zone (fissile fuel breeding zone, FEZ2) surrounding FEZ1 and including only ThO_2 fuel. The transmutation zones of both ADS designs are surrounded by reflector zone (RZ) and subsequently shield zone (SZ).

Figure 2 shows the cylindrical fuel rods cladded with zircaloy and located into the zones cooled with

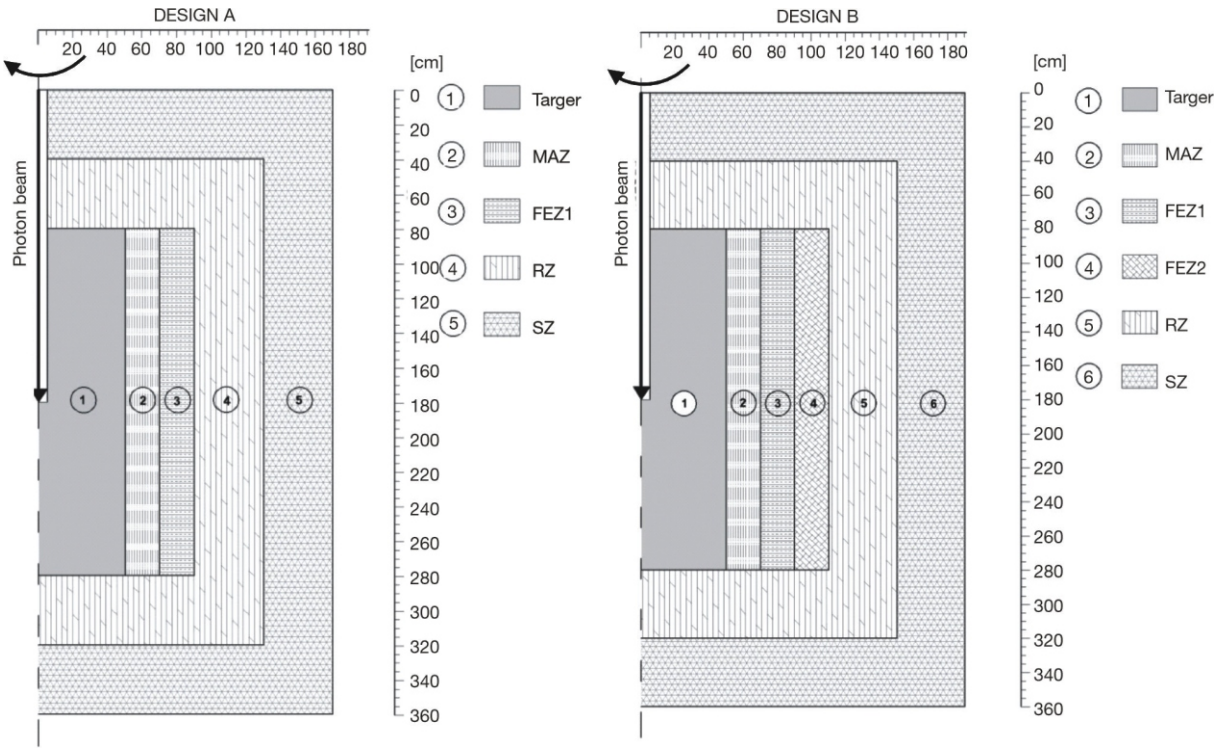

Figure 1. Axisymmetric vertical section views of MCNP models of the conceptual designed ADS

helium gas. Fuel rods are selected similarly to PWR fuel rods cladded with zircaloy [22]. Furthermore, in our subcritical studies, we prefer the hexagonal placement of the rods in the fuel zone. Pitch length (P) of cylindrical rods arrayed hexagonally is determined as 1.5 cm and 2 cm in the minor actinide zone (MAZ) and the fuel enrichment zones (FEZ), respectively. How this determination is made is described in the *Calculation procedure* subsection.

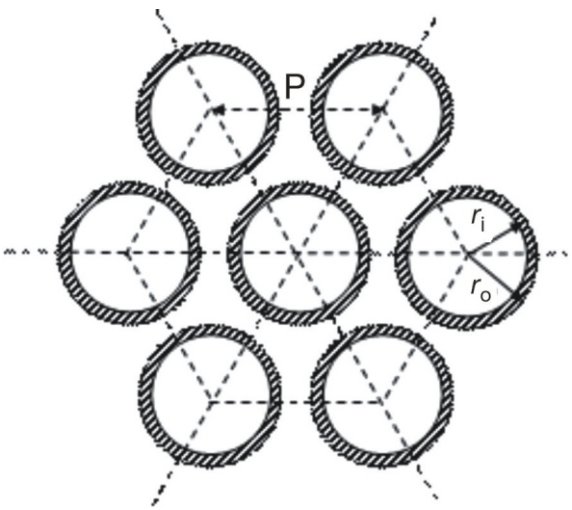

Figure 2. Hexagonal arrangement of the fuel rods in MAZ and FEZ (inner radius, r_i = 0.4699 cm and outer radius, r_o = 0.5461 cm

These dimensions are taken from ref. [22].

Depending on P, r_i, and r_o, the volumetric fractions (VF) of fuel, clad and coolant can be easily calculated with eqs. 1(a)-1(c). VF obtained from these calculations are given in tab. 1 as percentage.

$$VF_{\text{fuel}} \quad \frac{2\sqrt{3}}{3} r_i^2 \frac{1}{P^2} \; 100[\%] \tag{1a}$$

$$VF_{\text{clad}} \quad \frac{2\sqrt{3}}{3} (r_o^2 \quad r_i^2) \frac{1}{P^2} \; 100[\%] \tag{1b}$$

$$VF_{\text{coolant}} \quad 100 \quad VF_{\text{fuel}} \quad VF_{\text{clad}} \tag{1c}$$

Neutron-induced transmutation reactions

Neutron-isotope reaction chain and decay reactions, starting from ^{232}Th, are plotted in fig. 3. From this figure it can easily be observed which path the chain transformation (production or depletion) reactions of isotopes with atomic numbers greater than or equal to.

Table 1. Volume fractions

P [cm]	VF [%]		
	Fuel	Clad	Coolant
1.5	35.60	12.48	51.92
2.0	20.02	7.02	72.96

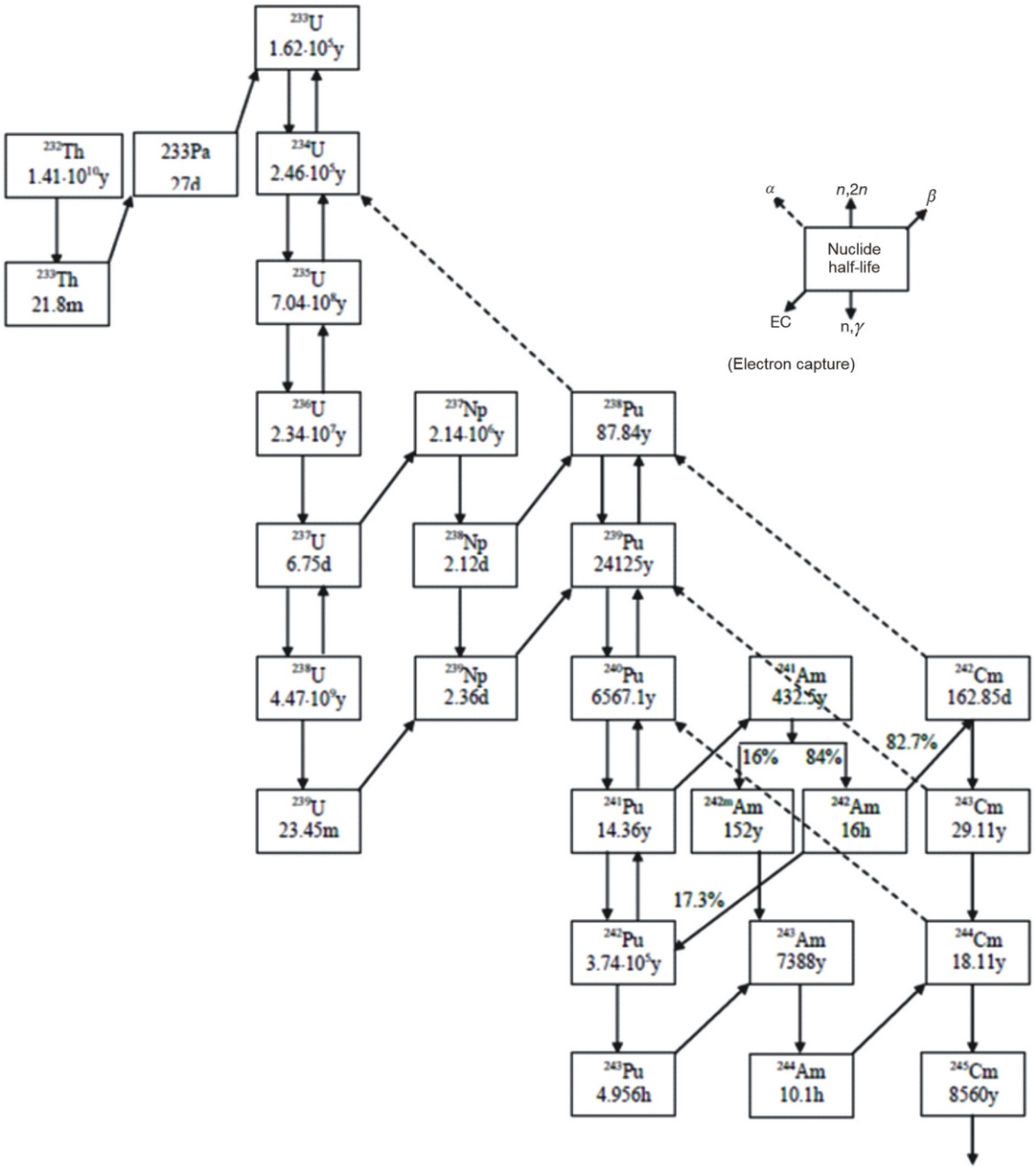

Figure 3. Neutron-isotope reaction chain and decay reactions starting from ^{232}Th

Spallation neutron target

In an ADS, the spallation neutron target is bombarded by high-energy protons, which in turn release many high energetic neutrons. The LBE is used in both ADS designs as the spallation neutron target material. The LBE alloy has very good chemical, neutronic, and thermal properties, and it, therefore, is one of the most widely used target materials in ADS applications, [23-29]. The proton energy, E_p, is assumed as 1000 MeV. To determine the optimum target radius, the performed numerical analyses, by changing target radius, bring out that 29.6 neutrons are released in LBE target having a radius of 50 cm by a single proton of 1000 MeV. This result is suitable with the literature [24, 28, 29], (see fig. 2 in [24]).

Sub-critical MAZ

The sub-critical zone of an ADS is fuelled with highly enriched fuels to obtain more energy gain, G, as well as effective transmutation of nuclear fuels. By fission reactions, this zone amplifies energy and increases the neutron population. In this study, two different MA compositions discharged from high burn-up PWR- MOX spent fuels [30] are separately used in both ADS designs. These MA compositions having a high fission capability like fissile fuels are denoted in [30] as MOX12 (33 GWd per tHM) and MOX22 (50 GWd per tHM), where tHM means tonnes of heavy metal.

Transmutation zone

In the transmutation zone of an ADS, radioactive isotopes in nuclear fuels can be transmuted into other isotopes by neutron-isotope reactions. Such as, fertile isotopes can be transmuted into fissile isotopes. In addition to these transmutations, if fissile isotopes exist sufficiently in the fuel, fission reactions can occur, and fission energy can be released. In other words, in the transmutation zone, a significant amount of energy can be produced as well as isotope transmutation obtained.

As is seen from fig. 1, the investigated ADS reactors, DESIGN A and DESIGN B, contain one and two FEZ, respectively.

DESIGN A:

In FEZ1, the fuel rods are individually filled with three different fuels in each case as follows:

– UO_2 extracted from CANDU spent fuel [31] (denoted as CANSF)
– UO_2 extracted from PWR spent fuel [32] (denoted as PWRSF),
– ThO_2 fuel

DESIGN B:

In the FEZ1, the fuel rods are filled separately with two different fuels in each case as

– CANSF
– PWRSF

The total of ten investigated cases including six different cases in DESIGN A and four different cases in DESIGN B are summarized in tab. 2.

Reflector zone

This zone is made of graphite being a good neutron reflector and moderator material for nuclear reactors. Moreover, graphite, having a high temperature resistant property, is a favoured material for nuclear reactor applications. The reflector zone reflects and returns the neutrons escaping from the sub-critical minor actinide and transmutation zones.

Table 2. Investigated MA composition and fuel cases

DESIGN	ZONE			
	MAZ		FEZ1	FEZ2
A	MA composition	MOX12	ThO_2	No zone
			CANSF	
			PWRSF	
		MOX22	ThO_2	
			CANSF	
			PWRSF	
B		MOX12	CANSF	ThO_2
			PWRSF	ThO_2
		MOX22	CANSF	ThO_2
			PWRSF	ThO_2

Shield zone

This zone is made of boron carbide (B_4C) having a very great ratio of the absorption cross-section to scattering cross-section. In nuclear reactor applications, B_4C is a favoured material for preventing neutron escape [33-36]. The shield zone absorbs neutrons escaping from the reflector zone thus preventing neutrons from going outside of the ADS.

In addition to the above explanations, densities and fractions of all isotopes used in the designed ADS are given in tab. 3. The atomic densities of isotopes can be easily calculated by using these data. The fuels are oxide materials.

CALCULATION TOOLS AND PROCEDURE

Calculation tools

To simulate nuclear processes in three dimensions, neutronic analyses are performed using the nuclear code MCNPX 2.7 [37], written by Los Alamos National Laboratory. Also, Los Alamos 150 MeV transport library (LA150) is used as a neutronic library. Chadwick *et al*. [38] developed this library for computational simulations

Table 3. Densities and fractions of isotopes used in the designed ADS

Material	Density [gcm^{-3}]	Isotopes	Fraction [%]	
TARGET				
LBE	11.344	Pb	44.5	
	9.8	Bi	55.5	
MINOR ACTINIDE ZONE			MOX12 [1]	MOX22 [1]
NpO_2	11.38	^{237}Np	4.5	4.4
		^{16}O		
AmO_2	11.50	^{241}Am	62.5	58.3
		^{243}Am	24.3	26.1
		^{16}O		
CmO_2	10.55	^{244}Cm	8.7	11.3
		^{16}O		
FUEL ENRICHMENT ZONES			CANSF [2]	PWRSF [3]
UO_2	10.974	^{234}U	$3.43822\cdot10^{-3}$	$2.02368\cdot10^{-2}$
		^{235}U	$1.66333\cdot10^{-1}$	$9.10655\cdot10^{-1}$
		^{236}U	$8.13407\cdot10^{-2}$	$3.84499\cdot10^{-1}$
		^{238}U	$9.97489\cdot10^{1}$	$9.86846\cdot10^{1}$
		^{16}O		
ThO_2	9.88	^{232}Th	100	
		^{16}O		
Coolant and Clad				
He	0.01648	^{4}He	100	
Zr	6.503	Zr	100	
REFLECTOR ZONE				
Graphite	2.1	^{12}C	100	
SHIELD ZONE				
B_4C	2.52	^{10}B	18.431	
		^{11}B	81.569	
		^{12}C		

of ADS. The time-dependent burnup/depletion cannot be calculated in ADS operating under sub-critic mode by MCNPX 2.7 code without an additional code. Therefore, in addition to this code and the LA150 library, the time-dependent burnup/depletion calculations are performed with the CINDER 90 computer code [39] integrated with MCNPX 2.7. To evaluate accurately the outputs of these codes, they are post-processed with CBURN [40] interface computer code.

Calculation procedure

Our previous studies [28, 29] bring out that maximum gain, G, is obtained when E_p is 1000 MeV. The numerical calculations, therefore, are performed for an E_p of 1000 MeV. A continuous uniform proton source, having a radius of 4 cm, bombards the target material (see fig. 1). The proton beam power of both conceptual ADS designs is assumed as 20 MW corresponding to $1.2483 \cdot 10^{17}$ protons having each an energy of 1000 MeV.

At the time-dependent neutronic analyses, to adjust the lowest effective neutron multiplication factor (k_{eff}) developing not under 0.90 at the beginning of the cycle (BOC), a series of calculations is carried out for the pitch length by numerical trial-and-error approach method. As a result of these calculations, the pitch lengths are determined as 1.5 cm and 2 cm in the MAZ and FEZ, respectively.

The time-dependent neutronic calculations are carried out until keffs reach up to 0.985 for all investigated cases, given in tab. 2, and thus the end of cycle (EOC) time is determined for each case as follows:

Determination of EOC times

Atomic densities are extracted for each intermediate period by means of CBURN interface computer code, using the final time-dependent results from MCNPX 2.7 and CINDER, then written as input to MCNPX2.7. By running MCNPX in critical calculation mode (with the KCODE option), keffs are calculated for each intermediate period. The EOC times determined by this way and being the longest operation times for all cases will be mentioned as the effective burn times in this study. The determined effective burn times by these processes are given in tab. 4. Furthermore, in this table, other important neutronic data obtained from the numerical calculations in both DESIGN A and B, also, are given as a summary.

Table 4. Summary table for the most important neutronic data obtained from the numerical calculations in DESIGN A and B

FEZ	MAZ	BOC EOC [d]	k_{eff}	Cumulative fuel enrichment, CFFE [%]			^{233}U [kg]	MA TF* [%]	G	BURNUP [GWd per MTU]**
				MAZ	FEZ1	FEZ2				
DESIGN A										
ThO_2	MOX12	0	0.904	91.21	0	–	0	–	0	0
		1250	0.985	86.12	3.07	–	104.783	9.21	10.8	25
	MOX22	0	0.910	88.59	0	–	0	–	0	0
		991	0.986	84.47	2.85	–	97.829	7.97	11.2	21
CANSF	MOX12	0	0.916	91.21	0.17	–	–	–	0	0
		920	0.985	86.68	2.76	–	–	7.98	18.4	29
	MOX22	0	0.927	88.59	0	–	–	–	0	0
		630	0.985	85.44	2.49	–	–	5.91	17.9	20
PWRSF	MOX12	0	0.943	91.21	0.91	–	–		0	0
		530	0.985	87.94	3.38	–	–	5.70	21.0	20
	MOX22	0	0.952	88.59	0	–	–	–	0	0
		300	0.985	86.37	2.95	–	–	4.07	25.1	14
	MOX22B***	300	0.939	87.36	0.91	–	–	–	0	0
		600	0.985	85.40	2.79	–	–	3.04	20.8	11
DESIGN B										
CANSF	MOX12	0	0.907	91.21	0.17	0	0	–	0	0
		2050	0.985	83.10	3.63	3.85	160.444	15.17	15.6	37
	MOX22	0	0.915	88.59	0.17	0	0	–	0	0
		1700	0.986	81.94	3.33	3.58	150.853	13.11	15.5	30
PWRSF	MOX12	0	0.913	91.21	0.91	0	0	–	0	0
		1950	0.985	83.41	4.23	3.84	160.673	14.56	15.4	35
	MOX22	0	0.922	88.59	0.91	0	0	–	0	0
		1600	0.985	82.09	3.99	3.58	151.183	12.97	16.0	30

* TF is transmutation fraction. The initial masses of MOX12 and MOX22 compositions are 5541.39 and 5550.08 kg, respectively.
** MTU stands for metric ton of uranium
*** At the second cycle (see the sections *Cumulative fissile fuel enrichment* and *Sample additional analysis*)

NUMERICAL RESULTS

Effective neutron multiplication factor

In nuclear reactors, the effective neutron multiplication factor, k_{eff}, being a very important parameter for the sustainability of reactor operation is described as the ratio of neutron numbers in one generation to neutron numbers in the preceding generation.

To obtain optimum neutronic values, both ADS designs are operated during the corresponding effective burn time of the case. As is apparent in tab. 4, while DESIGN A loaded with the MOX22 composition can be operated in the PWRSF case during the shortest effective burn time, 300 days, DESIGN B loaded with the MOX12 composition can be operated in the CANSF case during the longest effective burn time, 2050 days. Furthermore, in the same spent fuel cases in DESIGN B, the effective burn times in the MOX12 case are relatively long, about 1.2 times longer than those in the MOX22 case. This ratio varies from 1.26 to 1.77 in DESIGN A. In other words, in both designs, the cases fuelled with MOX12 composition have the effective burn time longer than those fuelled with MOX22 composition in all fuel cases. Moreover, it can be said that in general, in both designs, the effective burn times in the PWRSF cases are relatively shorter than those in the ThO_2 and CANSF cases. Briefly, these results point out that in all fuel and MA composition cases, DESIGN B can operate much longer than DESIGN A without new refuelling.

Figures 4(a) and 4(b) show the increases in keff in all fuel and MA cases in DESIGN A and B during the corresponding effective burn time of the case, respectively. One can see in these figs. that all keff profiles increase to 0.985. However, these increases are slightly curvilinear in DESIGN A *i. e.*, quasi-linear in DESIGN B.

Cumulative fissile fuel enrichment

The cumulative fissile fuel richness indicating the quality of nuclear fuel is defined as the ratio of the sum of atomic densities of fissile fuels to the sum of atomic densities of atoms with atomic numbers greater than or equal to 90.

In DESIGN A, the increases in CFFE values in all fuel and MA cases during the corresponding effective burn time of the case are plotted in fig. 5(a). As to DESIGN B, those in the MOX12 and MOX22 cases are separately plotted in fig. 5(b) and 5(c), respectively. As can be observed from these figures, all profiles of CFFE rise curvilinearly.

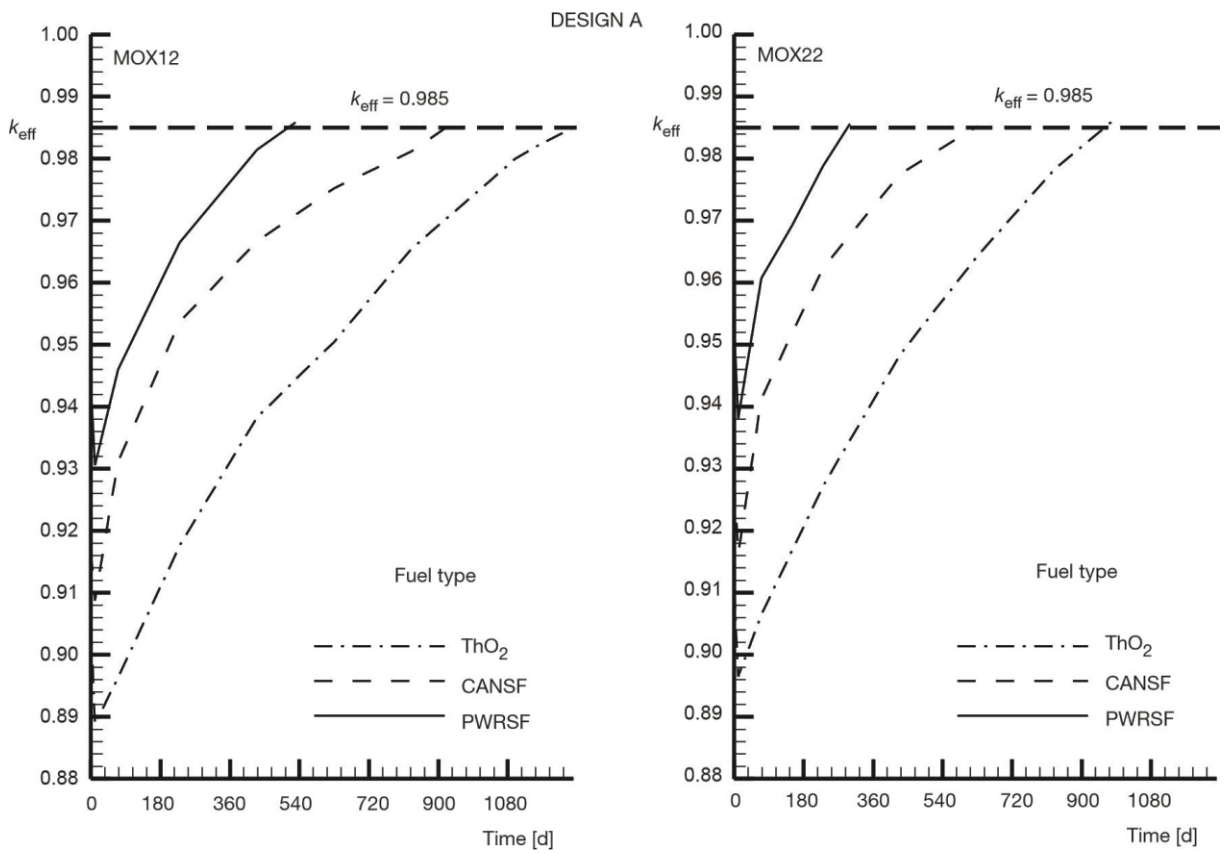

Figure 4(a). Increases in effective neutron multiplication factors in all fuel and MA cases during the corresponding effective burn time of the case

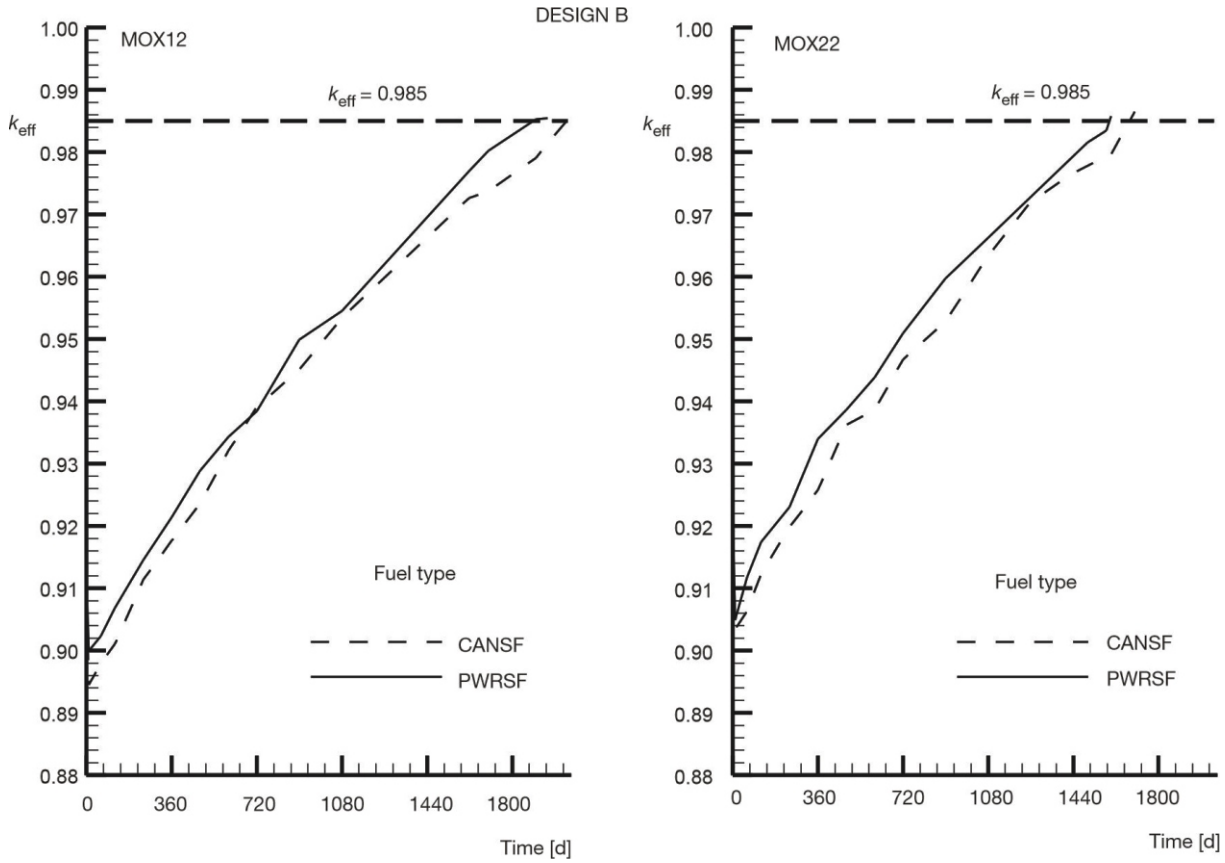

Figure 4(b). Increases in effective neutron multiplication factors in all fuel and MA cases during the corresponding effective burn time of the case

In addition to figs. 5(a)-5(c), the CFFE values in all investigated cases at the beginning and end of the cycle are given in tab. 4. In DESIGN A, the fuel enrichment processes in the ThO_2, CANSF, and PWRSF cases are individually conducted in one zone (FEZ1). While the CFFE values in the ThO_2, CANSF, and PWRSF cases rise to 3.07 %, 2.76 %, and 3.38 % in the MOX12 case, respectively, those rise to 2.85 %, 2.49 %, and 2.95 % in the MOX22 case, respectively. As to DESIGN B, unlike DESIGN A, the spent fuel enrichment and fissile fuel breeding are carried out simultaneously in two separate zones, FEZ1 and FEZ2.

These enrichments are as

- In FEZ1: While the CFFE values in the MOX12 case increase up to 3.63 % and 4.23 % in the CANSF and PWRSF cases, respectively, those in the MOX22 case increase up to 3.33 % and 3.99 %, respectively.
- In FEZ2: While the CFFE values in the MOX12 case cases increase up to 3.85 % and 3.84 % in the CANSF and PWRSF cases, respectively, those increase up to the same value, 3.58 %, in the MOX22 case.

As to MAZ, it is apparent from tab. 4, the CFFE values in this zone decrease on the contrary to those in FEZ1 and FEZ2 in all cases during their effective burn times. Depending on the MA composition and fuel type, the proportional amounts of these decreases vary between approximately 2.51 % with 5.58 % and 7.34 % with 8.89 % in DESIGN A and DESIGN B, respectively. As can be seen, the proportional decreases in CFFE in DESIGN B are greater than those in DESIGN A. The reason for this, DESIGN B is operated longer than DESIGN A. Moreover, the proportional decreases in CFFEs in MOX12 cases are greater than those in the MOX22 cases. Still, all CFFE values are high (above 80 %).

Transmutation fraction: The ratio of the net atomic density (N), transmuted during operation time (t), of an isotope to an atomic density of that at the BOC is defined as the transmutation fraction (TF). According to this definition, TF can be calculated as follows

$$TF \quad \frac{N(t) \quad N(0)}{N(0)} \tag{2}$$

The calculated total TF of MA compositions in this way are given in tab. 4. In DESIGN A, these fractions vary from 5.70 % to 9.21 % and from 4.07% to 7.97 % in the MOX22 and MOX12 cases depending on the fuel type, respectively. In DESIGN B, on the other hand, the ranges of change are noticeably short in the same cases and are from 15.4 % to 15.6 % and 15.5 % to 16 %, respectively. As is seen from these results, the TF values in DESIGN B are greater than in DESIGN A because of the longer effective burn times

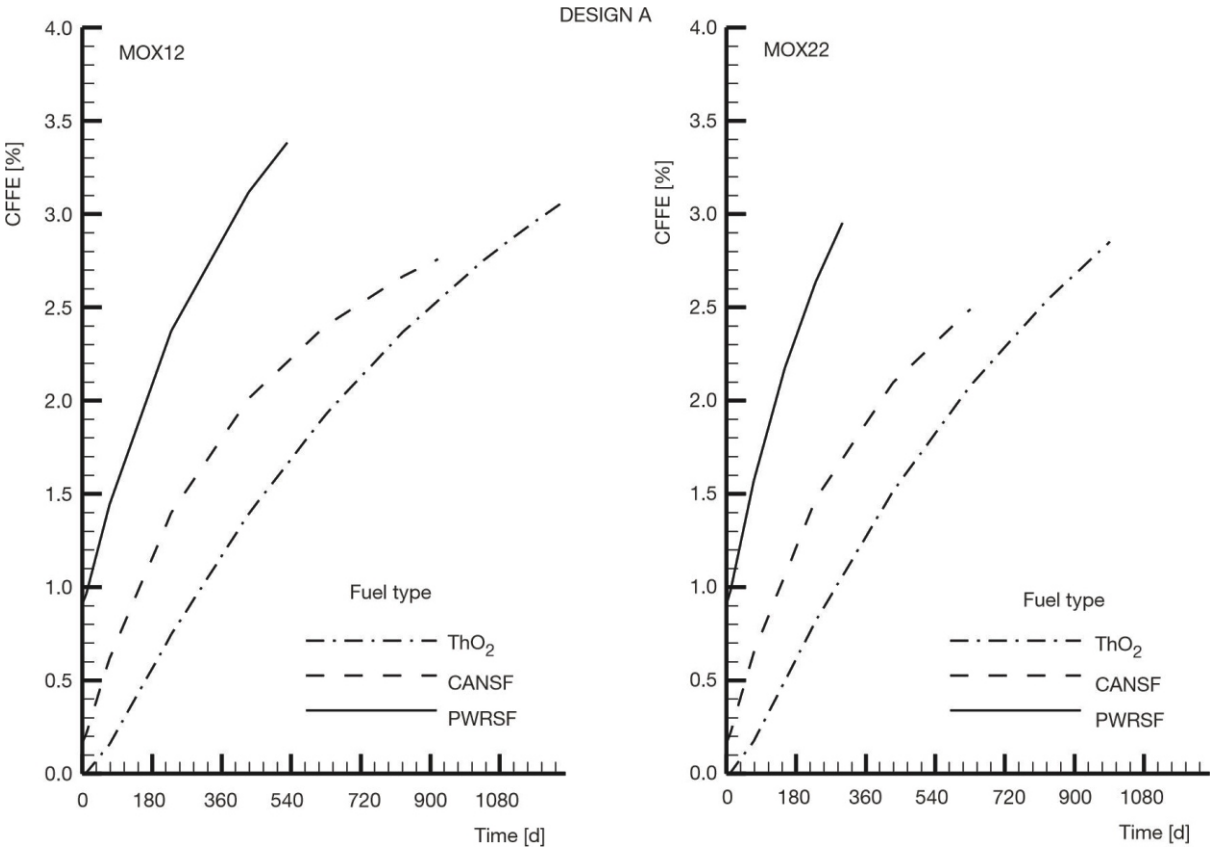

Figure 5(a). Increases in CFFE in all fuel and MA cases during the corresponding effective burn time of the case

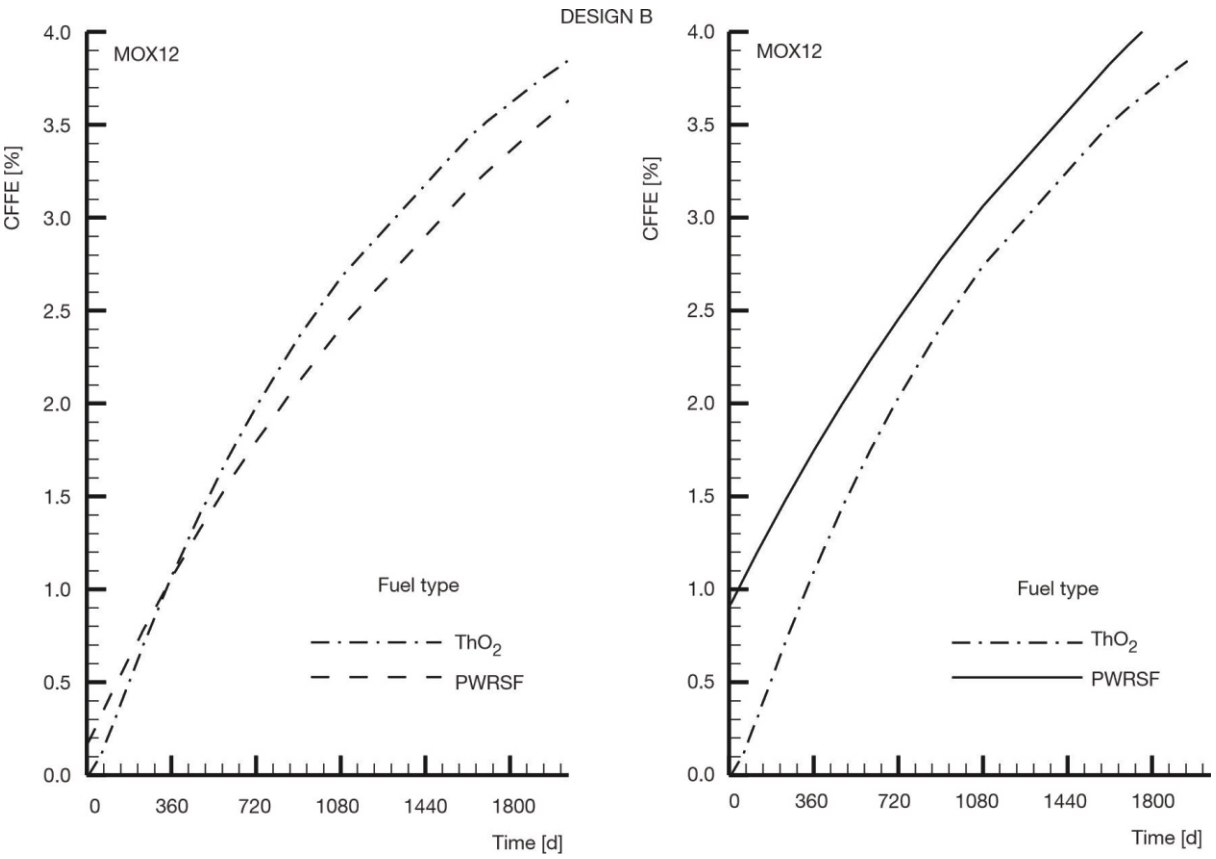

Figure 5(b). Increases in CFFE in all fuel and MOX12 cases during the corresponding effective burn time of the case

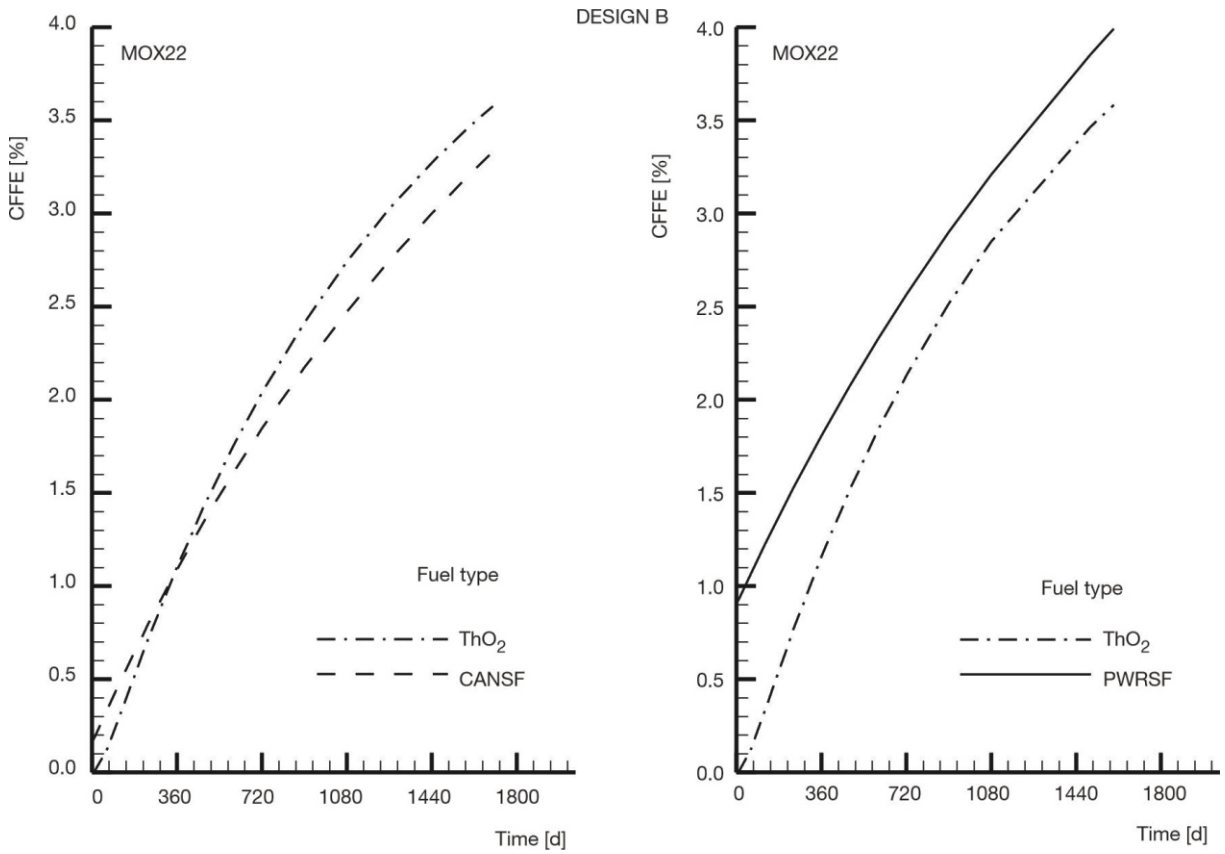

Figure 5(c). Increases in CFFE in all fuel and MOX22 cases during the corresponding effective burn time of the case

of DESIGN B. Furthermore, the MOX12 composition has a greater effect on fuel enrichment and fissile fuel breeding than the MOX22 composition.

The results bring out that the MOX12 composition has a more effect on the increase of CFFE than MOX22 composition in both designs as well as that the increases in CFFE in DESIGN B are higher than those in DESIGN A because DESIGN B has a longer effective burn time. Furthermore, the fuel enrichment and fissile fuel breeding processes are carried out simultaneously in two separate zones: the enrichment of spent fuels (CANSF and PWRSF) in FEZ1and the fissile fuel breeding from ^{232}Th in FEZ2This means DESIGN B may be more efficient than DESIGN A in terms of fuel enrichment and fissile fuel breeding.

The results of performed analyses bring out that in all fuel cases in DESIGN A, the enriched fuels, ThO_2, CANSF, and PWRSF, can be reused in PWR and CANDU reactors after an enrichment process of one or two years. As to DESIGN B, although an enrichment process of one year is sufficient for reusing of CANSF and ThO_2 in the CANDU reactor, an enrichment process of four years is required for reusing in PWR. Briefly, DESIGN A is more suitable than DESIGN B in terms of reusing the enriched fuels in short time.

Suggestions: We suggest that at the EOC, both reactors can continue to operate by removing only the enriched UO_2 and ThO_2 fuels from the reactors and replacing them with new spent UO_2 and ThO_2 fuels. Furthermore, at the EOC, the radioactive isotopes except for the isotopes of coolant and clad material occurring during the effective operation time and being not minor actinide must be taken out from the rods of burned MA compositions for obtaining high performance.

Energy gain

The energy gain, G, being one of the other important ADS parameters, is described as the ratio between the total energy produced by fission reactions in the ADS per proton to E_p, and calculated as follows

$$G \quad \frac{R_f E_f}{E_p} \tag{3}$$

where R_f and E_f are the numbers of fission reactions and energy amount released from one fission reaction (200 MeV), respectively.

Figures 6(a) and 6(b) show the increases in G in all fuel and MA cases in DESIGNs A and B during the corresponding effective burn time of the case, respectively. All G profiles rise quasi-linearly. Moreover, in DESIGN A, the G profiles in the PWRSF and CANSF cases rise more sharply with respect to ThO_2 cases Also, as is apparent in tab. 4, while the values of G in DESIGN A at the EOC vary in a wide range of 10.8 and 25.1 depending on the

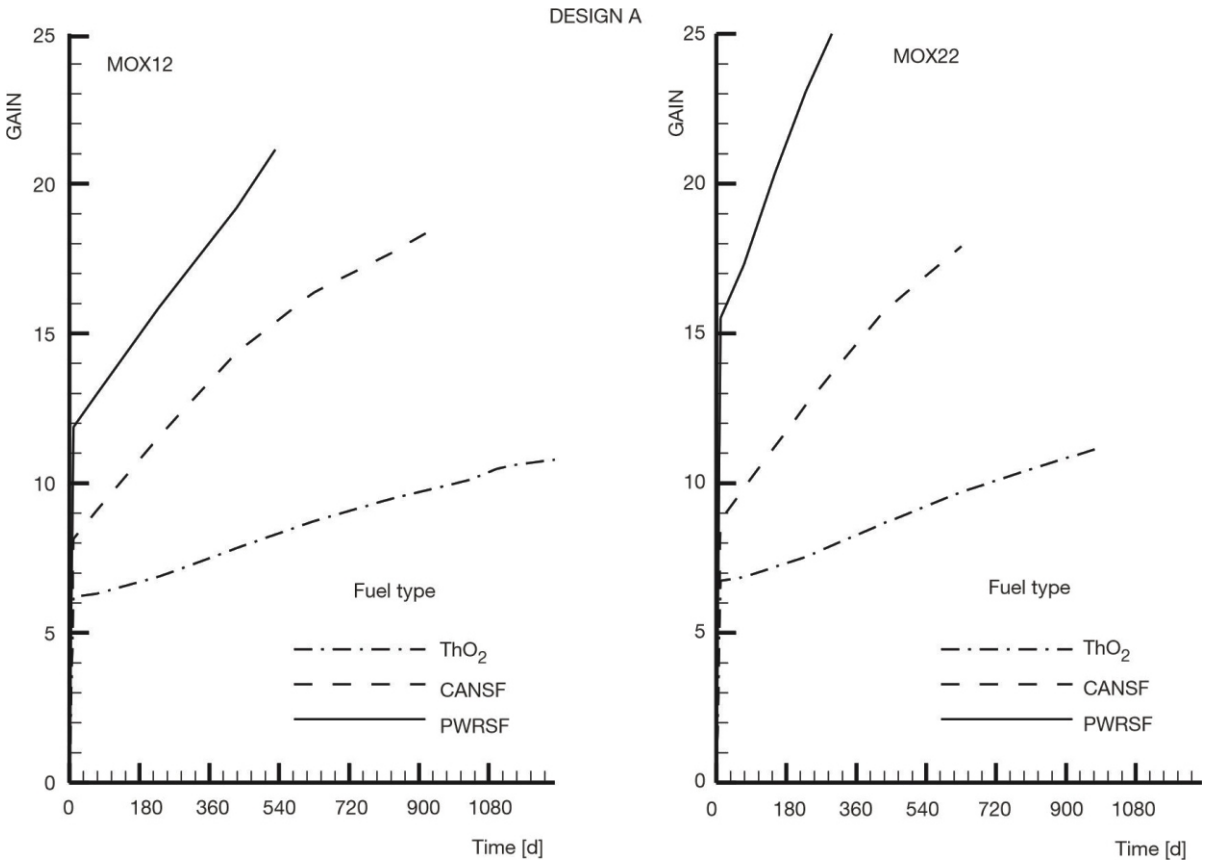

Figure 6(a). Increases in gain in all fuel and MA cases during the corresponding effective burn time of the case

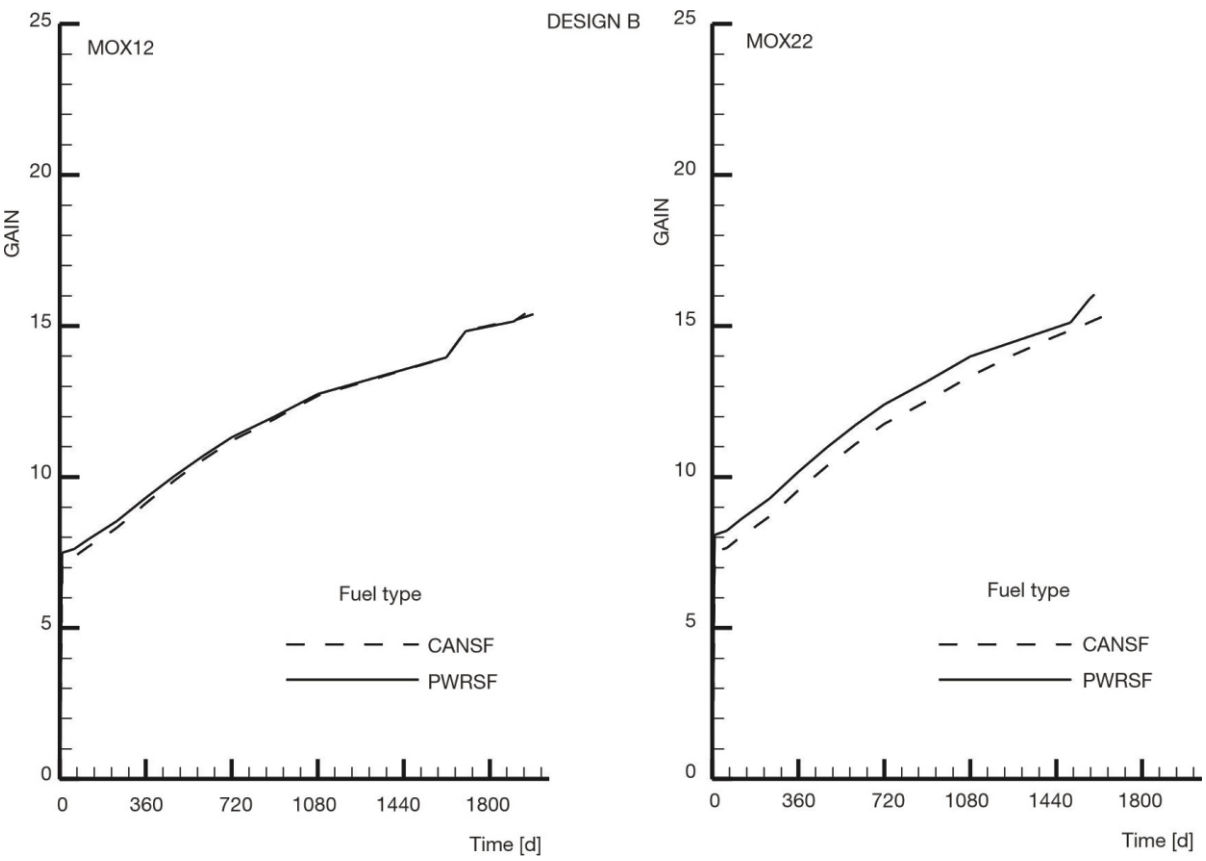

Figure 6(b). Increases in gain in all fuel and MA cases during the corresponding effective burn time of the case

MA composition and fuel type, these values are around 15-16, and relatively lower in DESIGN B than in DESIGN A. This means that DESIGN A has more performance than DESIGN B in terms of energy multiplication.

Thorium utilization

In a nuclear reactor core including ^{232}Th isotopes, if these isotopes react with neutrons under favourable conditions, they transform into the fissile ^{233}U isotopes with two consecutive negative beta (electron) emissions after 27 days as follows

$$\begin{array}{ccccc} {}^{232}\mathrm{Th} & \mathrm{n} & \gamma & {}^{232}\mathrm{Th} & 21.83\ \mathrm{min} \\ {}^{233}\mathrm{Pa} & \beta & 27\ \mathrm{days} & {}^{233}\mathrm{U} & \beta \end{array} \tag{4}$$

In this study, to analyse in detail the thorium utilization and, accordingly, the fissile ^{233}U production, a total of six cases containing ThO_2, two cases in DESIGN A and 4 cases in DESIGN B, are considered. Figures 7(a) and 7(b) depict the increase in the ratios of mass of ^{233}U, produced from ^{232}Th, to a mass of ^{232}Th in all cases of fuel and MA compositions in DESIGN A and B during the corresponding effective burn time of the case, respectively. One can see from these figures, that in both designs, the profiles of these ratios rise curvilinear in all fuel and MA composition cases, and

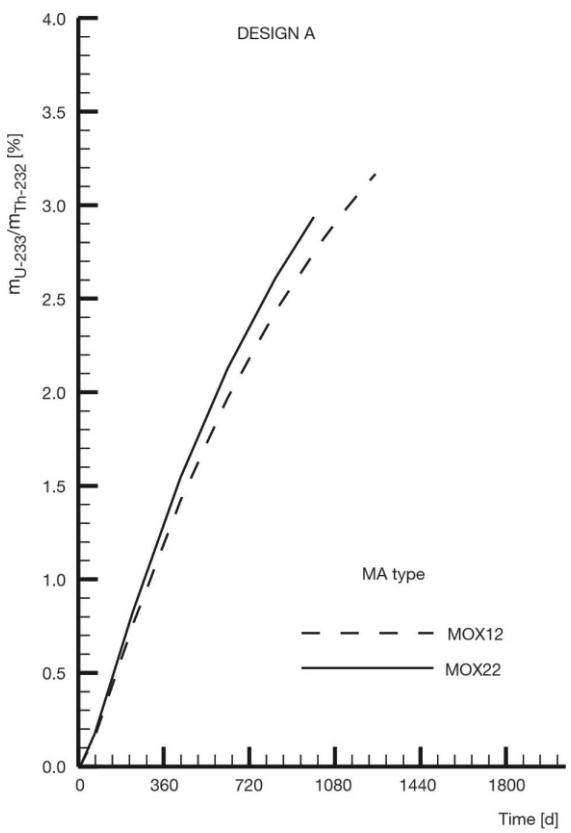

Figure 7(a). Increases in ratios mass of ^{233}U to mass of ^{232}Th in all cases of fuel and MA compositions during the corresponding effective burn time of the case

that the MA composition and fuel differences do not significantly affect ratio profiles in the same design. In DESIGN A, the mass ratio profiles reach up to 3.17 % and 2.94 % in the MOX12 and MOX22 cases, respectively. These values are slightly higher (approximately 30 %) in DESIGN B, namely, the mass ratio profiles reach up to about 4 % and 3.7 % in the MOX12 and MOX22, respectively.

In addition to the mass ratio profiles, at EOC, the masses of produced ^{233}U in all investigated cases are pointed in tab. 4 as kg. The initial masses of ^{232}Th are 3495.80 kg and 4369.74 kg in DESIGN A and B, respectively. While the produced ^{233}U accumulates up to about 105 kg and 98 kg in MOX12 and MOX22 cases in DESIGN A, respectively, that accumulates up to about 160 kg and 150 kg in the same MA composition cases in DESIGN B. The reason for this high difference is that the initial mass of ^{232}Th in DESIGN B is greater than that in DESIGN A, (approximately 25 %). While the mass of ^{232}Th in DESIGN B is only 1.25 times greater than that in DESIGN A, the ^{233}U production in DESIGN B is 1.5 times greater than that in DESIGN A because the transmutation time in DESIGN B is longer than that in DESIGN A. This means that DESIGN B has a higher ^{233}U production performance than DESIGN A in terms of the produced mass.

Fuel burnup

Another important parameter in ADS is fuel burnup which is indicated as the total produced energy per unit metric fuel mass loaded in the beginning, and its unit is expressed mostly as GWd per MTU or MWd per MTU. The fuel burnup can be calculated depending on the operation time and fission energy released in ADS as follows

$$\mathrm{BURNUP}\,(t \quad t) \quad \mathrm{BURNUP}\,(t) \quad \frac{\text{Fission Power}}{\mathrm{MTU}} \quad t \tag{5}$$

where MTU is metric ton of uranium.

Figures 8(a) and 8(b) present the accumulations of the BURNUP in all cases of fuel and MA composition in DESIGN A and B during the corresponding effective burn time of the case, respectively. As is seen from these figures the profiles of BURNUP quasi-linearly rise in all investigated cases. One can see that, while the fuel type very much affects BURNUP profiles in DESIGN A, these profiles are hardly or not affected in both fuel and MA composition cases in DESIGN B.

In DESIGN A, while BURNUPs in MOX12 accumulate up to about 25, 29, and 20 GWd per MTU in the ThO_2, CANSF, and PWRSF cases at EOC, respectively, those in MOX22 accumulate up to 21, 20, and 14 GWd per MTU, respectively. As to DESIGN B, while BURNUP in MOX12 accumulate up to about 37

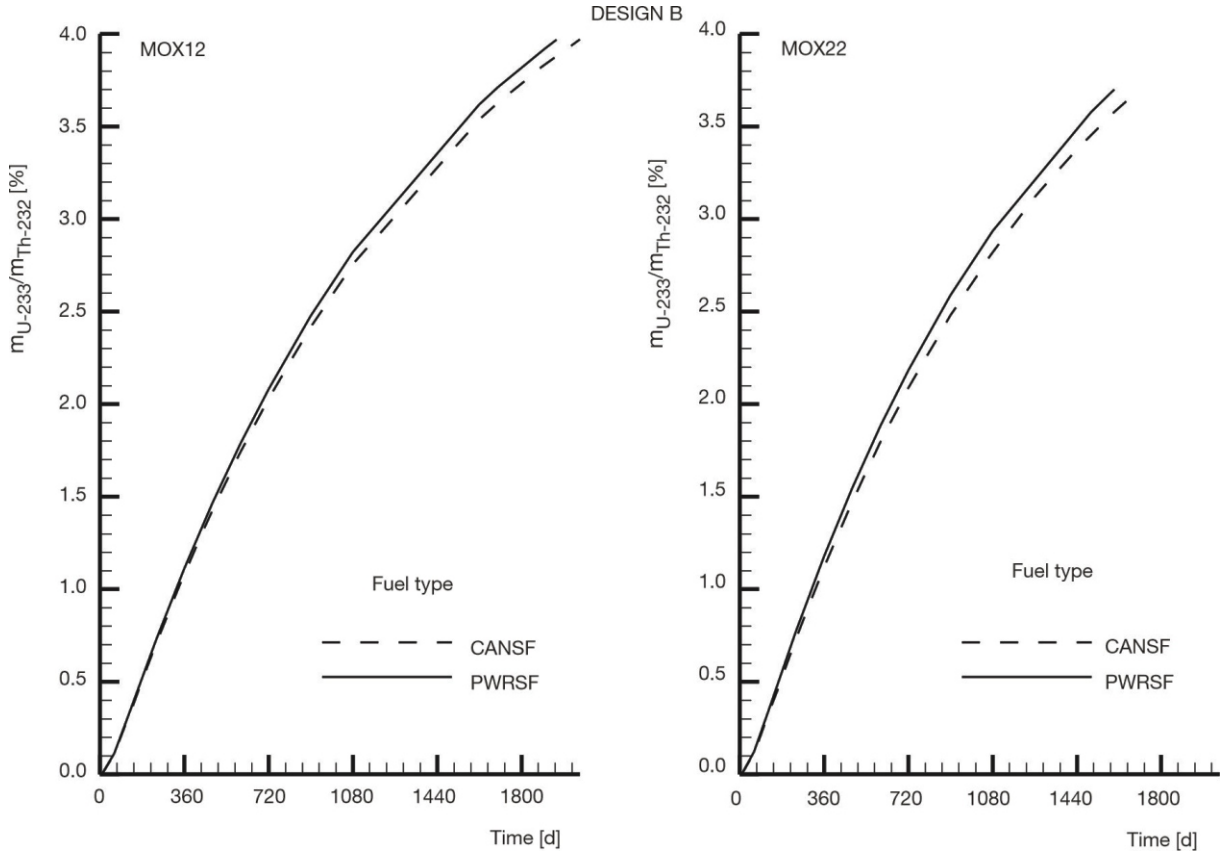

Figure 7(b). Increases in ratios of mass of ^{233}U to a mass of ^{232}Th in all cases of fuel and MA compositions during the corresponding effective burn time of the case

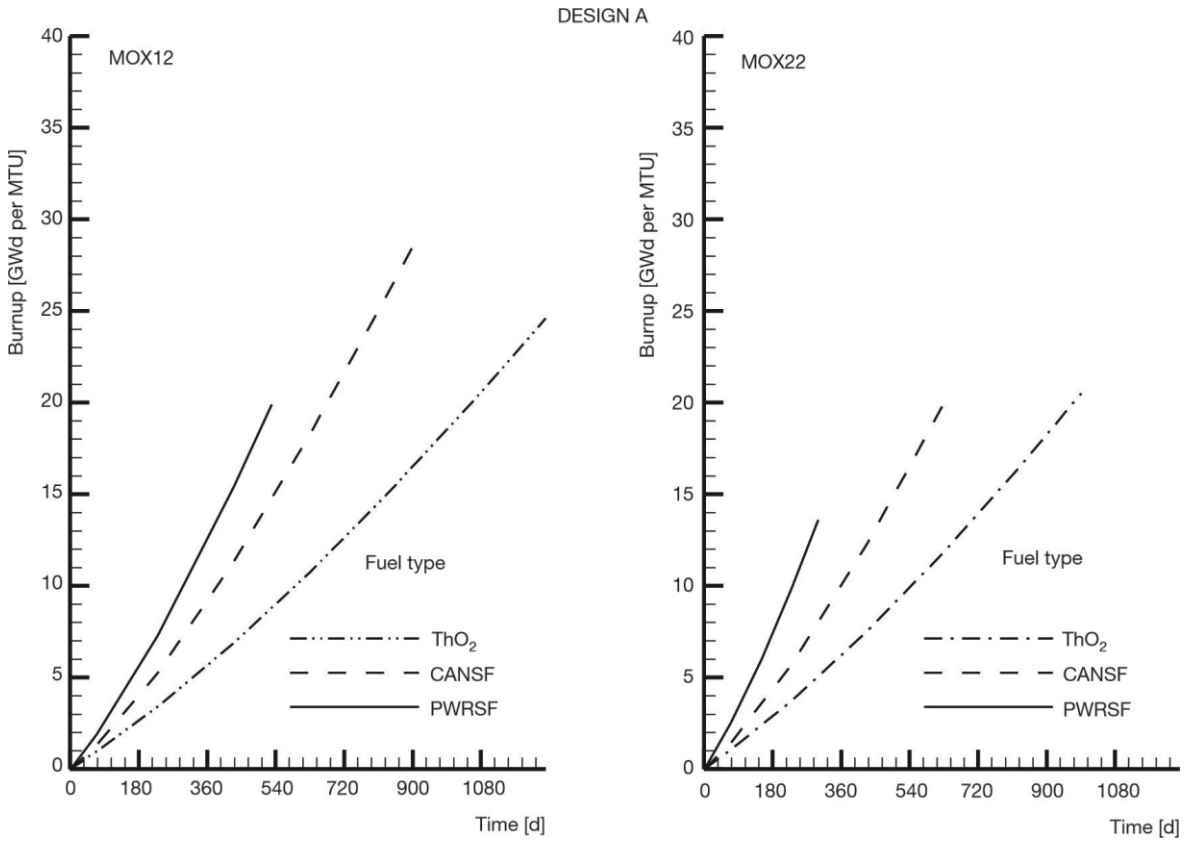

Figure 8(a). Accumulation of BURNUP in all fuel and MA cases during the corresponding effective burn time of the case

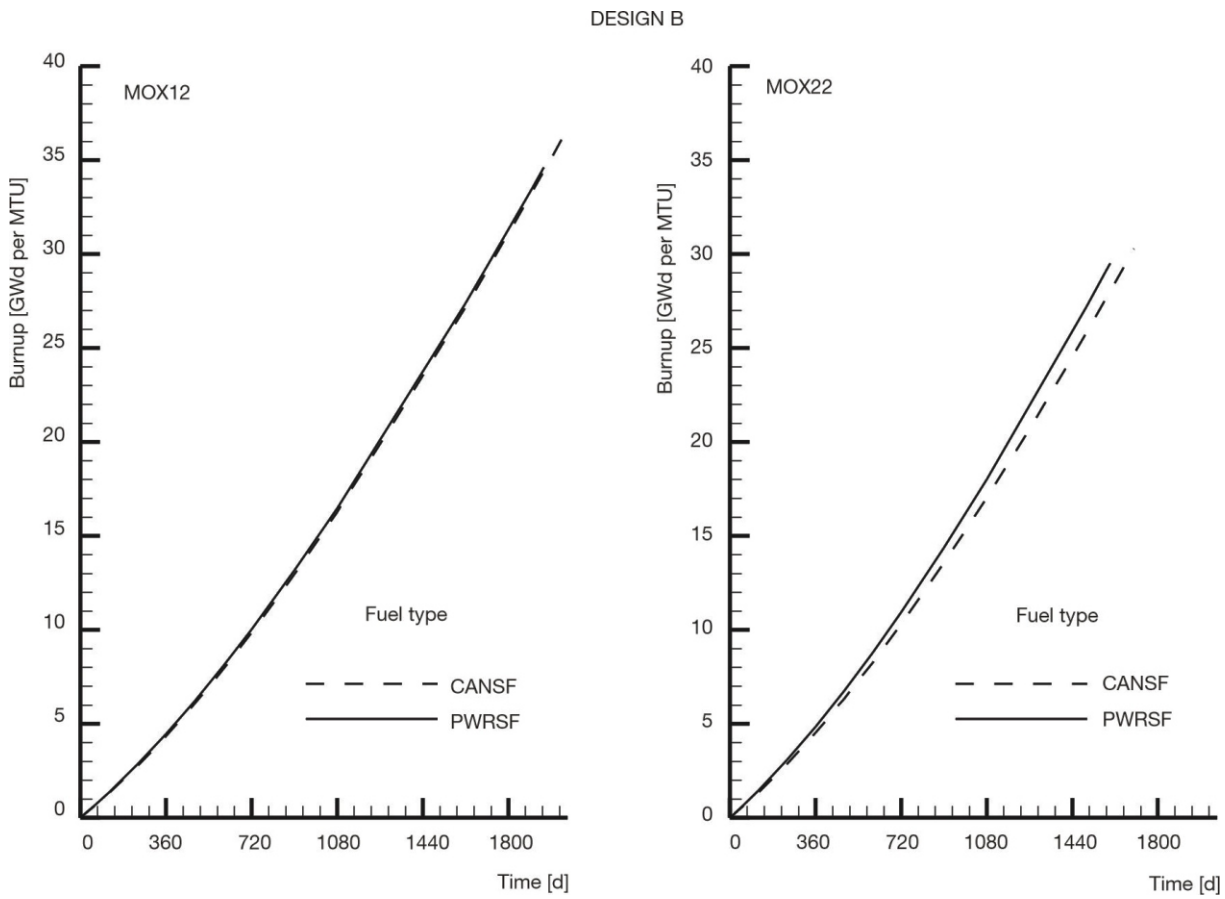

Figure 8(b). Accumulation of BURNUPs in all fuel and MA cases during the corresponding effective burn time of the case

and 35 GWd per MTU in the CANSF and PWRSF cases, respectively, at EOC, those in MOX22 increase to about 30 GWd per MTU in both fuel cases. As expected, the BURNUP values in DESIGN B are higher than in DESIGN A due to DESIGN B having a longer effective burn time.

Sample additional analysis

In line with our suggestion, sample analysis is performed by refuelling as described in section 4.2 for the case of MOX22 and PWRSF in DESIGN A. This burned MA composition is denoted as MOX22B. The neutronic data from this analysis, also, are given in tab. 4. At the end of the second cycle, the k_{eff} value reaches up to 0.985 again in 300 days. Meanwhile, the CFFE value rises to 2.79 % and an additional, total MA transmutation of 3.04 % is obtained. However, this TF is 25 % lower than in the 1st cycle. The values G and BURNUP, also, are approximately 20 % lower than in the 1st cycle. In brief, the significant amounts of fuel enrichment and MA transmutation take place in the 2nd cycle, albeit at 20-25 % lower performance than in the 1st cycle.

CONCLUSIONS

To perform the enrichment of CANDU and PWR spent fuels, as well as the production of fissile fuel from thorium, two different ADS with one and two transmutation zones and fuelled with the MA compositions are designed conceptually. Two different MA compositions are individually used in the core of both ADS designs as fuel. The neutronic analysis results obtained from ten different fuel enrichment and fissile fuel production cases, formed this way in the ADS, are presented briefly below.

In both ADS designs, the MOX12 composition makes a greater positive effect on the neutronic values than the MOX22 composition.

In DESIGN A, the lowest and highest effective burn times are 300 days and 1250 days. These times are 1600 and 2050 days in DESIGN B. This means that DESIGN B can operate much more time than DESIGN A without refuelling.

In DESIGN A, the enriched fuels, ThO_2, CANSF, and PWRSF, can be reused in PWR and CANDU reactors after an enrichment process of 1 or 2 years. In DESIGN B, although an enrichment process of 1 year is sufficient for reusing of CANSF

and ThO_2 in the CANDU reactor, an enrichment process of 4 years is required for reusing in PWR.

While energy gain in DESIGN A at EOC varies in a wide range of 10.8 and 25.1 depending on the MA composition and fuel type, this value is relatively lower, around 15-16 in DESIGN B than DESIGN A.

In DESIGN A, the ratios of mass of ^{233}U, produced from ^{232}Th to mass of ^{232}Th, reach up to 3.17 % and 2.94 % in the MOX12 and MOX22 cases, respectively. In DESIGN B, these ratios reach up to about 4 % and 3.7 % in the same MA cases.

The BURNUP values quasi-linearly increase to 21 and 37 GWd per MTU in DESIGN A and B, respectively.

Consequently, both ADS reactors have a good neutronic performance and can produce a significant amount of energy, as well as enriching spent fuel and producing fissile fuel from thorium.

As known, nuclear waste management is one of the most important issues for nuclear power plants. ADS can be a solution to these waste problems. We would like to emphasize that the results of this study will contribute to the solution of nuclear waste management and will light the way for designs of ADS consuming and transmuting minor actinide hold out in the spent fuels of conventional thermal reactors as well as energy production. At the same time, the uranium fuels in the spent fuels and thorium fertile fuels would be enriched in the ADS without using any fresh fissile fuel (enriched uranium, plutonium, *etc*.,).

AUTHORS' CONTRIBUTIONS

Theoretical and numerical analyses were conducted by B. Durmaz, A. B. Arslan, G. Bakir, and H.Yapici analyzed and discussed the results. The manuscript was written and the figures prepared by all authors.

REFERENCES

[1] Rubbia, C., *et al*., Conceptual Design of a Fast Neutron Operated High Power Energy Amplifier, *European Organization for Nuclear Research,* (1995), pp. 95-44

[2] Gohar, Y., *et al*., ADS Design Concept for Disposing of the U.S. Spent Nuclear Fuel Inventory, *Annals of Nuclear Energy, 160* (2021), 9, 108385

[3] Yapici, H., Study on Transmutation of Minor Actinides Discharged from High Burn-Up PWR-MOX Spent Fuel in the Force-Free Helical Reactor, *Annals of Nuclear Energy, 30* (2003), 4, pp. 413-436

[4] Yapici, H., Burning and/or Transmutation of Transuraniums Discharged from PWR-UO_2 Spent Fuel and Power Flattening Along the Operation Period in the Force Free Helical Reactor, *Energy Conversion and Management, 44* (2003), 18, pp. 2893-2913

[5] Yapici, H., Determination of the Optimal Plutonium Fraction in Transuranium Discharged from Pressured Water Reactor (PWR) Spent Fuel for a Flat Fission Power Generation in the Force-Free Helical Reactor (FFHR) along the Transmutation Period, *Annals of Nuclear Energy, 30* (2003), 6, pp. 633-649

[6] Yapici, H., *et al*., Minor Actinide Transmutation Potential of Modified PROMETHEUS Fusion Reactor, *Journal of Fusion Energy, 23* (2004), 2, pp. 121-135

[7] Yapici, H., *et al*., Neutronic Analysis for Transmutation of Minor Actinides and Long-Lived Fission Products in a Fusion-Driven Transmuter (FDT), *Journal of Fusion Energy, 25* (2006), 3-4, pp. 225-239

[8] Yapici, H., *et al*., Transmutation-Incineration Potential of Transuraniums Discharged from PWR-UO_2 Spent Fuel in Modified PROMETHEUS Fusion Reactor, *Fusion Engineering and Design, 81* (2006) 18, pp. 2093-2108

[9] H. Y., Yang, *et al*., Physical Studies of Minor Actinide Transmutation in the Accelerator-Driven Subcritical System, *Nucl Sci Tech, 30* (2019), 91

[10] Rodriguez I. M., *et al*., The Nuclear Fuel Cycle Code ANICCA: Verification and a Case Study for the Phase Out of Belgian Nuclear Power with Minor Actinide Transmutation, *Nuclear Engineering and Technology, 52* (2021), 10, pp. 2274-2284

[11] Liu, B., *et al*., Minor Actinide Transmutation in the lead-Cooled Fast Reactor, *Progress in Nuclear Energy, 119* (2020), 103148

[12] Liu, B., *et al*., Minor Actinide Transmutation Characteristics in AP1000, *Annals of Nuclear Energy, 115* (2018), pp. 116-125

[13] Zhou, S., *et al*., Flexibility of ADS for Minor Actinides Transmutation in Different Two-Stage PWR-ADS Fuel Cycle Scenario, *Annals of Nuclear Energy, 111* (2018), pp. 271-279

[14] Arslan, A. B., *et al*., Transmutations of Long-Lived and Medium-Lived Fission Products Extracted from CANDU and PWR Spent Fuels in an Accelerator-Driven System, Science and Technology of Nuclear Installations, *Science and Technology of Nuclear Installations, 13* (2019)

[15] Bakir, G., Genc, G., Yapici, H., Time-Dependent Neutronic Analysis of a Power-Flattened Gas Cooled Accelerator Driven System Fuelled with Thorium, Uranium, Plutonium, and Curium Dioxides TRISO Particle, *Science and Technology of Nuclear Installations, 11* (2016), https://doi.org/10.1155/2016/2612459

[16] Bakir, G., Yapici, H., Analysis of Fuel Rejuvenation Times in a Fusion Breeder Reactor Fuelled with a Mixture of Uranium-Thorium Oxides for the CANDU Reactor, *Nucl Technol Radiat, 32* (2017), 3, pp. 193-203

[17] Ali, A. M. M., *et al*., Study of Different Seed Fuels with Thorium in Accelerator-Driven Subcritical System, *Nuclear Science and Engineering, 195* (2021), 2, pp. 203-213

[18] Kral, D., *et al*., Investigation of Thorium Utilization in Accelerator Driven Systems, 19th International Scientific Conference on Electric Power Engineering (EPE), 2018, 66

[19] Zhu, G., *et al*., Thorium Utilization with Pebble Mixing System in Fluoride Salt-Cooled High Temperature Reactor, *Progress in Nuclear Energy, 114* (2019), 4, pp. 413-436

[20] Yang, P., *et al*., Preliminary Neutron Study of a Thorium-Based Molten Salt Energy Amplifier, *Nuclear Science and Techniques, 30* (2020), 4, pp. 413-436

[21] Qaaod, A. A. Al., *et al*., Computational Study on Distribution Feasibility of Radioactive Waste Transmutation in Accelerator Driven System, *Nucl Technol Radiat, 35* (2020), 4, pp. 294-303

[22] Allen, K. S., Advancad Polymeric Burnable Poison Rod Assemblies for Pressurized Water Reactors, University of Florida, 2003

[23] Ding, H., *et al*., Verification and Application of SuperMC3.3 to Lead-Bismuth-Cooled Fast Reactor, *Nucl Technol Radiat, 34* (2019), 2, pp. 122-128

[24] Nema, P. K., Application of Accelerators for Nuclear Systems: Accelerator Driven System (ADS), *Energy Procedia, 7* (2011), Dec., pp. 597-608

[25] Sugawara, T., *et al*., Transient Analysis for Lead-Bismuth-Cooled Accelerator-Driven System, *Annals of Nuclear Energy, 55* (2013), May, pp. 238-247

[26] Tsujimoto, K., *et al*., Neutronics Design for Lead-Bismuth Cooled Accelerator Driven System for Transmutation of Minor Actinide, *Journal of Nuclear Science and Technology, 41* (2004), 1, pp. 21-36
[27] ***, Accelerator And Spallation Target Technologies for ADS Application, Nuclear Science, a Status Report, 2005
[28] Yapici, H., *et al*., Neutronic Limits in Infinite Target Mediums Driven by High Energetic Protons, *Annals of Nuclear Energy, 34* (2007), 5, pp. 374-384
[29] Yapici, H., *et al*., A Comprehensive Study on Neutronics of a Lead-Bismuth Eutectic Cooled Accelerator-Driven Sub-Critical System for Long-Lived Fission Product Transmutation, *Annals of Nuclear Energy, 35* (2008), 7, pp. 1264-1273
[30] ***, NEA, Calculations of Different Transmutation Concepts an International Benchmark Exercise (Nuclear Science Committee, 2000)
[31] Tait, J. C., *et al*., Validation of the ORIGEN-S Code for Predicting Radionuclide Inventories in Used CANDU Fuel, *Journal of Nuclear Materials, 223* (1995), 2, pp. 109-121
[32] Zhiwen, Xu, *et al*., Impact of High Burnup on PWR Spent Fuel Characteristics, *Nuclear Science and Engineering, 151* (2005), 3, pp. 261-273
[33] Chen, Z., *et al*., Nuclear Waste Transmutation Performance Assessment of an Accelerator Driven Subcritical Reactor for Waste Transmutation (ADS-NWT), *Annals of Nuclear Energy, 75* (2015), Jan., pp. 723-727
[34] Cinotti, L., *et al*., The experimental Accelerator Driven System (XADS) Designs in the EURATOM 5th Framework Programme, *Journal of Nuclear Materials, 335* (2004), 2, pp. 148-155
[35] Kiani, M. A., *et al*., Preparation and Characteristics of Epoxy/Clay/B4C Nanocomposite at High Concentration of Boron Carbide for Neutron Shielding Application, *Radiation Physics and Chemistry, 141* (2017), pp. 223-228
[36] Li, X., *et al*., High Temperature Resistant Polyimide/Boron Carbide Composites for Neutron Radiation Shielding, *Composites Part B: Engineering, 159* (2019), Feb., pp. 355-361
[37] Pelowitz, D. B., MCNPX User's Manual, Version 2.7.0, LA-CP-11-00438, Los Alamos Scientific Laboratory, 2011
[38] Chadwick, M. B., *et al*., Cross-Section Evaluations to 150 MeV for Accelerator-Driven Systems and Implementation in MCNPX, *Nuclear Science and Engineering, 131* (1999), 3, pp. 293-328
[39] Wilson, W. B., Cowell, S. T., Manual for CINDER'90 Version 07.4 Codes and Data, LA-UR-07-8412, Los Alamos Scientific Laboratory 2007, Version 07.4.2, updated, 2018
[40] Yapici, H., CBURN Interface Computer Code for Evaluation of Time-Dependent CINDER90 Outputs, Erciyes University, Turkey, 2018

Received on September 24, 2021
Accepted on February 21, 2022

Бушра ДУРМАЗ, Гизем БАКИР, Алпер Бугра АРСЛАН, Хусејин ЈАПИЦИ

НЕУТРОНСКА АНАЛИЗА СИСТЕМА ПОКРЕТАНОГ АКЦЕЛЕРАТОРОМ НАПАЈАНИМ МИНОРНИМ АКТИНИДОМ И ДИЗАЈНИРАНИМ ЗА ОБОГАЋИВАЊЕ ИСТРОШЕНОГ ГОРИВА И ПРОИЗВОДЊУ ФИСИБИЛНОГ ГОРИВА

У раду је приказана анализа обогаћивања уранијума извађеног из истрошених горива CANDU и PWR реактора, и добијање фисионог горива из торијума у два хелијумом хлађена система покретана акцелераторима различитих дизајна: ДИЗАЈН А и ДИЗАЈН Б. На почетку, проценти ^{235}U у уранијумским горивима, извађеним из истрошених горива CANDU и PWR реактора, износе 0.17 % и 0.91 %, респективно. Оба акцелератором покретана језгра напајају се са два минорна актинида различитог састава екстрахованих из PWR-MOX истрошеног горива. ДИЗАЈН А има једну зону трансмутације (зону обогаћивања) која окружује горивно језгро и садржи горива од торијума или истрошеног уранијума, док ДИЗАЈН Б има другу зону трансмутације (зону обогаћивања фисибилног горива) која окружује прву зону трансмутације и која садржи само торијумско гориво. Укратко, анализирано је укупно 10 случајева формираних комбинацијама дизајна акцелератора, компонентама минорних актинида и истрошеним уранијумом са торијумским горивима, а то чини шест случајева у ДИЗАЈНУ А који садржи једну трансмутациону зону и четири у ДИЗАЈНУ Б који садржи две трансмутационе зоне. Еутектичка легура олово-бизмут, течни тешки метал, који се састоји од 45 % олова и 55 % бизмута, користи се као материјал мета у испитиваном акцелератором покретаном систему. Претпоставља се да је мета бомбардована са 1.2383 10^{17} протона у секунди и да је енергија сваког протона 1000 MeV. Што значи да је снага протонског снопа 20 MW. Тродимензионалне и временски зависне неутронске анализе спроведене су коришћењем MCNPX 2.7 и CINDER 90 нуклеарног кода. Оба дизајна система раде све док k_{eff} не достигну вредност 0,985, да би се одредила најдужа радна времена која су ефективна времена сагоревања у свим служајевима.
У зависности од дизајна, састава минорног актинида и типа горива (утрошени UO_2 и ThO_2), резултати добијени на крају циклуса показују да ефективно време изгарања варира од 300 дана до 2050 дана, обогаћење горива може достићи 2.49-4.23 % и вредности добитка у енергији 10.8-25.1.

Кључне речи: систем покретан акцелератором, термички реактор, обогаћивање утрошеног горива, коришћење торијума